 CMES, vol.3, no.6, pp.791-801, 2002

Dynamic Response of 3-D Damaged Solids and Structures by BEM

G.D. Hatzigeorgiou[1] **and D.E. Beskos**[1]

Abstract: This paper presents a general boundary element methodology for the dynamic analysis of three-dimensional inelastic solids and structures. Inelasticity is simulated with the aid of the continuum damage theory. The elastostatic fundamental solution is employed in the integral formulation of the problem and this creates in addition to the surface integrals, volume integrals due to inertia and inelasticity. Thus an interior discretization in addition to the usual surface discretization is necessary. Isoparametric linear quadrilateral elements are used for the surface discretization and isoparametric linear hexahedra for the interior discretization. Advanced numerical integration techniques for singular and nearly singular integrals are employed. Houbolt's step-by-step numerical time integration algorithm is used to provide the dynamic response. Numerical examples are presented to illustrate the method and demonstrate its accuracy.

keyword: Dynamic response, damage mechanics, boundary element method, three-dimensional structures.

1 Introduction

Dynamic analysis of linear elastic structures by either the finite element method (FEM) or the boundary element method (BEM) has reached a rather mature state of development [Zienkiewicz and Taylor (1991), Beskos (1997), Kogl and Gaul (2000)]. In recent years, intensive research has been carried out to develop reliable numerical methods for determining the nonlinear behavior of various types of structures under dynamic loading. The FEM is the most popular numerical method for the solution of dynamic inelastic problems involving two- and three-dimensional (2-D and 3-D) solids and structures [Zienciewicz and Taylor (1991)]. Recently, the BEM has emerged as a reliable alternative method of solution of this class of problems, as it is evident in the book of Banerjee (1994) and in the review articles of Beskos (1995) and Providakis and Beskos (1999).

The BEM in its direct conventional form and in conjunction with the elastostatic fundamental solution of the problem has been successfully used for the analysis of 2-D elastoplastic solids and structures under static [Telles and Brebbia (1979)] and dynamic loading [Carrer and Telles (1992), Kontoni and Beskos (1993), Providakis and Beskos (1994), Telles and Carrer (1994)]. The first 3-D dynamic elastoplastic analysis by the BEM was very recently presented by Hatzigeorgiou and Beskos (2002a). The BEM in its symmetric Galerkin form and in conjunction with the elastostatic fundamental solution of the problem has also been successfully applied to static [Maier and Pollizzotto (1987)] and dynamic [Frangi and Maier (1999)] inelastic problems in a 2-D space. The BEM in its direct conventional form and in conjunction with the elastodynamic fundamental solution of the problem has the advantage of restricting the interior discretization to those parts of the domain expected to become inelastic, but is very complicated due to the need for satisfying causality at every time step. [Ahmad and Banerjee (1989), Telles, Carrer and Mansur (1999)]. Furthermore, use of the elastodynamic fundamental solution may create problems of instability [Siebrits and Peirce (1997)]. Inelasticity, especially for quasi-brittle materials can be successfully and very simply simulated by continuum damage theories [Krajcinovic (1996), Bazant and Planas (1998)].

It is worth noticing that the applications of BEM to analyze damaged structures are restricted only to static problems. The first application of BEM in combination with damage mechanics originated by Rajgelj, Amadio and Nappi (1992) and then extented by Herding and Kuhn (1996), Sellers and Napier (1997), Cerrolaza and Garcia (1997), Garcia, Florez-Lopez and Cerrolaza (1999), to 2-D structures under static loading. Furthermore, the first 3-D static BEM implementation of damage analysis was very recently established by Hatzigeorgiou and Beskos (2002b). Thus, the need for the development of an accu-

[1] Department of Civil Engineering, University of Patras, 26500, Patras, Greece.

rate and efficient BEM for the analysis of 3-D damaged structures under dynamic loading is apparent.

In this paper a general boundary element methodology is developed for the analysis of three-dimensional inelastic solids and structures under static and dynamic loads. The method employs the elastostatic fundamental solution of the problem because of its simplicity. This creates volume integrals due to inertia and inelasticity in addition to the boundary ones. Thus, an interior discretization is necessary in addition to the boundary one. Inelasticity is simulated in this work by damage theory, which is used for reproducing nonlinear behavior of brittle materials, like concrete or rock, in a simple, yet very successful way. The matrix equations of motion are numerically integrated in time with the aid of Houbolt's algorithm. Three numerical examples serve to illustrate the method and demonstrate its accuracy.

2 Boundary Element Formulation

For a three-dimensional body Ω which is bounded by its surface Γ, the Somigliana identity for the dynamic inelastic case associated to the initial stress formulation is defined as

$$\begin{aligned} c_{ij}u_j(\xi,t) &= \int_\Gamma u^*_{ij}(\xi,X)p_j(X,t)d\Gamma(X) - \\ &\int_\Gamma p^*_{ij}(\xi,X)u_j(X,t)d\Gamma(X) - \\ &\int_\Omega \rho u^*_{ij}(\xi,X)\ddot{u}_j(X,t)d\Omega(X) + \\ &\int_\Omega \varepsilon^*_{jki}(\xi,X)\sigma^p_{jk}(X,t)d\Omega(X) \end{aligned} \tag{1}$$

In the above, t is the time, ρ the constant mass density of the body, c_{ij} the usual free coefficient of elastostatic analysis and $u^*_{ij}(\xi,X)$, $p^*_{ij}(\xi,X)$ and $\varepsilon^*_{jki}(\xi,X)$ are the fundamental solution components of the elastostatic problem representing the displacement, traction and strain, respectively. Furthermore, u_j, $\ddot{u}_j$, p_j and σ^p_{jk} represent the displacements, accelerations, tractions and inelastic stresses, respectively. Eq. (1) represents the equation of motion of the body in integral form. For $\rho = 0$ this equation reduces to the static case. In order to solve Eq. (1), the boundary element method (BEM) is applied. The boundary of the 3-D body is discretized to NB linear quadrilateral boundary elements and the domain is discretized to NV linear hexahedral volume cells (see Fig. 1).

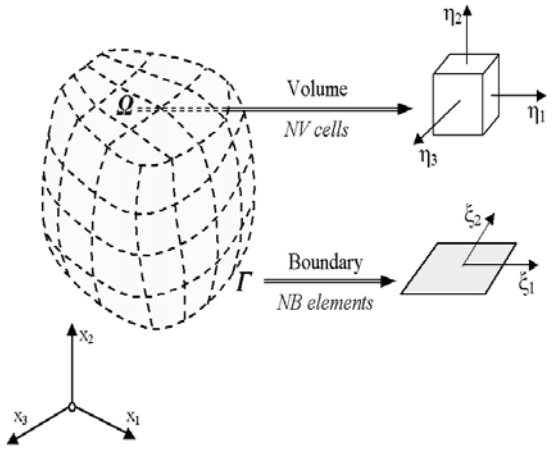

Figure 1 : Discretization of a general three-dimensional body

Then, Eq. (1) becomes

$$\begin{aligned} c_{ij}u_j(\xi,t) &= \sum_{m=1}^{NB}\left\{\int_{\Gamma m} u^*_{ij}(\xi,X)\Phi d\Gamma\right\}p_j(X,t) - \\ &\sum_{m=1}^{NB}\left\{\int_{\Gamma m} p^*_{ij}(\xi,X)\Phi d\Gamma\right\}u_j(X,t) - \\ &\sum_{n=1}^{NV}\left\{\int_{\Omega n} \rho u^*_{ij}(\xi,X)\Phi d\Omega\right\}\ddot{u}_j(X,t) + \\ &\sum_{n=1}^{NV}\left\{\int_{\Omega n} \varepsilon^*_{jki}(\xi,X)\Phi d\Omega\right\}\sigma^p_{jk}(X,t) \end{aligned} \tag{2}$$

where Φ is the matrix of the shape functions. Eq. (2) is rewritten in a compact form as

$$\begin{aligned} c_{ij}u_j &= \sum_{m=1}^{N_{BE}} G_{ij}p_j - \sum_{m=1}^{N_{BE}} H_{ij}u_j - \\ &\sum_{n=1}^{N_{VC}} M_{ij}\ddot{u}_j + \sum_{n=1}^{N_{VC}} Q_{ij}\sigma^p_{jk} \end{aligned} \tag{3}$$

The boundary element implementation transforms the

system of integral equations to an equivalent algebraic system, which in matrix notation reads

$$[G]\{p(t)\} - [H]\{u(t)\} - [M]\{\ddot{u}(t)\} + [Q]\{\sigma^p(t)\} = \{0\} \quad (4)$$

In Eq. (4) matrices [G] and [H] correspond to the boundary integrals and [M] and [Q] to the inertial and initial stress domain integrals, respectively. The construction of the above matrices requires integrations in every element and cell as described in Eq. (2). Regular and nearly singular integrals are evaluated by the standard Gaussian quadrature. The computation of nearly singular integrals requires an increased number of Gauss points to reduce the numerical error into a low level. Thus, an empirical relation proposed by Bu (1997) is adopted to achieve a controlled relative error less than 0.1%. This relation reads

$$N_k \geq 1 + 2.1 \left(\frac{d_{\min}}{L_k} \right)^{-0.8} \quad (5)$$

where N_{min} is the minimum number of Gauss points for each element, d_{min} the minimum distance between the collocation point and the element and L_k the length of the element side to the integration direction. Singular integrals are evaluated by the Guiggiani and Gigante method [Guiggiani and Gigante (1990)]. The main advantage of this method is its simplicity. The application of Guiggiani & Gigante method requires the execution of two steps. In the first one, a transformation of coordinates from local Cartesian to an equivalent polar system for boundary elements and to a spherical system for volume cells is applied. This step causes a complete suppression of the singularities of [G], [M] and [Q] matrices appearing in Eq. (4). In the second step, a Taylor expansion of the remaining singularities of the [H] matrix at length leads to a regular integrand.

3 Computation of response

The Houbolt scheme is selected for the integration in time because it gives excellent results with respect to stability and accuracy. Thus, the acceleration is expressed in displacement terms as (Karabalis &Beskos 1997)

$$\ddot{u}_{n+1} = \frac{1}{\Delta t^2}(2u_{n+1} - 5u_n + 4u_{n-1} - u_{n-2}) \quad (6)$$

If the current time step is the $(n+1)$, substitution of Eq.(6) into Eq.(4) gives

$$\Delta t^2[G]\{p_{n+1}\} - (\Delta t^2[H] + 2[M])\{u_{n+1}\} = [M]\{-5u_n + 4u_{n-1} - u_{n-2}\} - \Delta t^2[Q]\{\sigma^p_{n+1}\} \quad (7)$$

or in a compact form

$$[G^*]\{p_{n+1}\} - [H^*]\{u_{n+1}\} = [M]\{u^*\} - [Q^*]\{\sigma^p_{n+1}\} \quad (8)$$

where

$$[G^*] = \Delta t^2[G],\ [H^*] = \Delta t^2[H] + 2[M],\ [Q^*] = \Delta t^2[Q] \text{ and } u^* = -5u_n + 4u_{n-1} - u_{n-2} \quad (9)$$

The assumption of zero initial displacement, velocity and initial stress gives the initial conditions

$$[G]\{p_0\} - [M]\{\ddot{u}_0\} = \{0\} \quad (10)$$

Use of the boundary conditions enables one to solve the above equation and obtain the initial tractions and accelerations. After the application of the boundary conditions, Eq. (8) becomes

$$[GH]\left\{ \begin{array}{c} p \\ u \end{array} \right\}_{n+1} = [M]\{u^*\} - [Q^*]\{\sigma^p_{n+1}\} + \{B\} \quad (11)$$

where $[GH]$ corresponds to the $[G^*]$ and $[H^*]$ terms, while $\{B\}$ arises from the known boundary conditions. The tractions and displacements in the left-hand side cannot be computed from Eq. (11) because of the ignorance of the stress vector $\{\sigma_p\}$ in the right hand side. The solution of this equation requires an iterative procedure. The computation of stresses via the way "displacements $\rightarrow$ strains $\rightarrow$ stresses" (see Fig. 2) is selected because it is more efficient than the computation via integral equations, which requires much more computational effort [Banerjee (1994)]. The iterative scheme employed here is an extension of Banerjee's static inelastic iterative algorithm [Banerjee (1994)] to dynamics. In every time step, starting with the assumption of an elastic structure, the solution of Eq. (11) gives the first estimation for displacements and tractions. From these displacements, the strains are obtained and use of the constitutive equation, described in the next section, enable one to determine the elastic, inelastic and total stresses. The inelastic stresses in Eq. (11) give a second estimation for displacements and tractions etc. If convergence is satisfied in this procedure, the next time step follows. The solution procedure appears in Fig. 3.

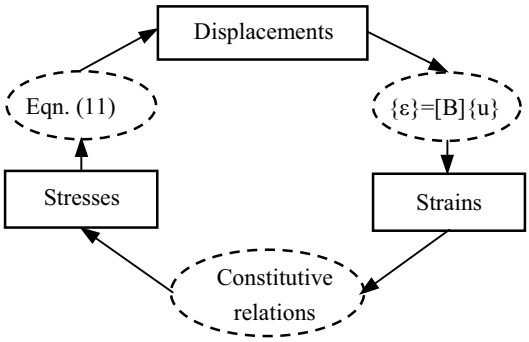

Figure 2 : Iterative procedure for the computation of stresses

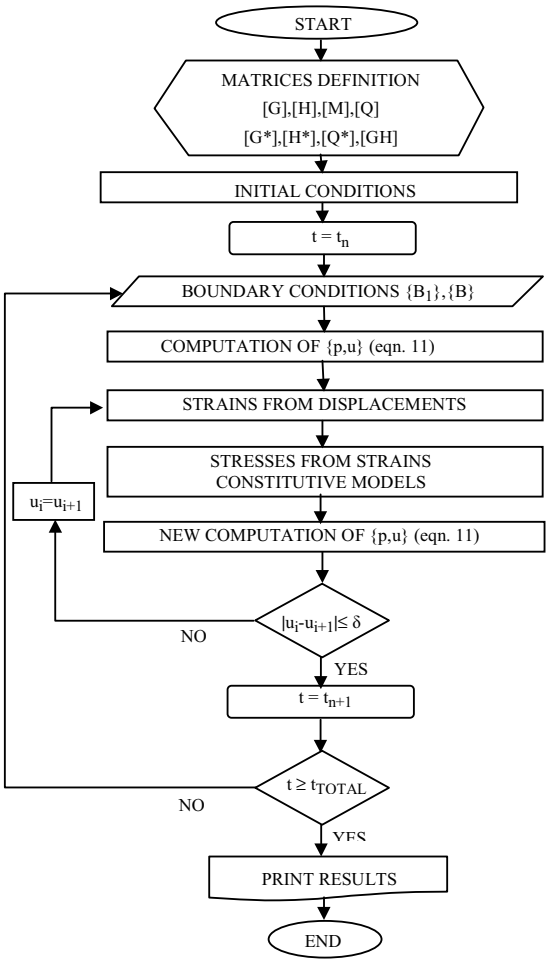

Figure 3 : Solution algorithm

4 Material modeling

This paper is mainly concerned with brittle materials like concrete, rock, soil and ceramics. The non-linear behavior of these materials presents some common characteristics that damage theory is ideal to simulate [Krajcinovic (1996)]. In this paper the Oñate (1997) and a modified Faria-Oliver(1993)/Mazars (1986) - FOM damage models are adopted to describe the main characteristics of brittle materials. The FOM model consists of the elastic-damage part of the plasticity-damage model of Faria and Oliver expressed in terms of the tension and compression damage indices, which are combined to produce a suitable average damage index on the basis of a Mazars' type theory. The Oñate and FOM models take into account the different response of material under tension and compression states and the effect of stiffness degradation. In order to clarify the concept of elastic isotropic damage, a section of the body with overall area S_n, effective resisting area $\overline{S}_n$ and area of the voids $(S_n - \overline{S}_n)$ is considered. The damage index d is defined as

$$d = \frac{S_n - \overline{S}_n}{S_n} = 1 - \frac{\overline{S}_n}{S_n} \tag{12}$$

The equilibrium relationship between the standard Cauchy stress σ and the effective stress $\overline{\sigma}$ gives $\sigma S_n = \overline{\sigma}\overline{S}_n$and thus in view of Eq (12), the constitutive equation can be written as

$$\{\sigma\} = (1-d)\{\overline{\sigma}\} = (1-d)[C]\{\varepsilon\} \tag{13}$$

where $[C]$ is the elastic constitutive matrix. The analysis requires the knowledge of the damage index d and its evolution at every stage of the deformation process. The described below constitutive models satisfy this demand.

4.1 Oñate's model

The application of Oñate's model requires the determination of the norm of strain state, τ, the damage criterion and the damage index evolution.

The norm of strain state, τ, results from

$$\tau = \left(\theta + \frac{1-\theta}{n}\right)\left[\{\overline{\sigma}\}^T [C]^{-1} \{\overline{\sigma}\}\right]^{1/2} \tag{14}$$

where n is the compressive to tensile strength ratio

$$n = \left(\frac{f_c}{f_t}\right) \tag{15}$$

and θ is given by

$$\theta = \frac{\sum_{i=1}^{3} <\overline{\sigma}_i>}{\sum_{i=1}^{3} |\overline{\sigma}_i|} \tag{16}$$

The symbol (<>) corresponds to MacAuley brackets where

$$\langle \pm\overline{\sigma}_i \rangle = \frac{1}{2}\left(|\overline{\sigma}_i| \pm \overline{\sigma}_i\right) \tag{17}$$

The damage criterion is given by

$$F(\tau - r) = \tau - r \leq 0 \tag{18}$$

where

$$r = \max\left(\frac{f_t}{\sqrt{E}}, \tau\right) \tag{19}$$

Finally, the evolution of the damage index d results from

$$d = 1 - \frac{r^o}{r}\exp\left[A^+\left(1 - \frac{r}{r^o}\right)\right] \tag{20}$$

where

$$A^+ = \left(\frac{G_f E}{l^* f_t^2} - \frac{1}{2}\right)^{-1} \tag{21}$$

with G_f being the fracture energy, E the modulus of elasticity and l^* an internal length scale. The last parameter provides response independent of mesh discretization. Cervera, Oliver and Faria (1995) proposed the relation

$$l_j^* = \sqrt[3]{V_j} \tag{22}$$

to determine the characteristic length l^*, where V is the volume of the j-internal element (volume cell). The stress-strain diagram in uniaxial conditions and the damage bounding surface in biaxial conditions of Oñate's model appear in Fig. 4. It is obvious that this model cannot take into account the biaxiality effect in compression.

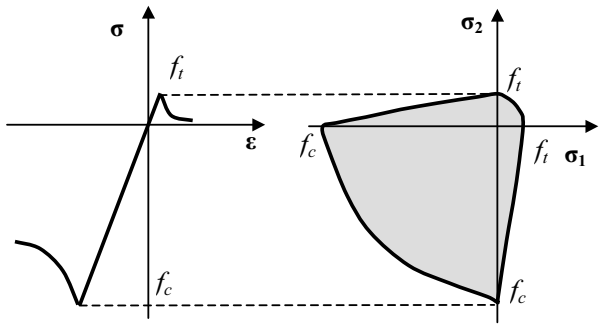

Figure 4 : Oñate's model representation

4.2 FOM model

The application of FOM model requires the following 5 steps:

Step1

Compute the effective strains from the principal strains ε_i by

$$\begin{array}{ll} <\varepsilon_i> = \varepsilon_i & >\varepsilon_i <= 0 \\ <\varepsilon_i> = 0 & >\varepsilon_i <= \varepsilon_i \end{array} \quad \text{and} \quad \begin{array}{l} \text{when} \\ \end{array} \quad \begin{array}{l} \varepsilon_i > 0 \\ \varepsilon_i \leq 0 \end{array} \tag{23}$$

Compute the equivalent strains from

$$\tilde{\varepsilon}^+ = \sqrt{\sum_{i=1}^{2} <\varepsilon_i>^2} \text{ and } \tilde{\varepsilon}^- = \sqrt{\sum_{i=1}^{2} >\varepsilon_i <^2} \tag{24}$$

$$\hat{\varepsilon}^+ = \sqrt{\max\left(<\varepsilon_i>\right)/\sum_{i=1}^{3} <\varepsilon_i>} \quad \text{and}$$

$$\hat{\varepsilon}^- = \sqrt{\min\left(>\varepsilon_i<\right)/\sum_{i=1}^{3} >\varepsilon_i <}$$

Step2

Compute the effective stresses from the principal elastic stresses $\overline{\sigma}_i$ from

$$\begin{array}{ll} <\overline{\sigma}_i> = \overline{\sigma}_i & >\overline{\sigma}_i <= 0 \\ <\overline{\sigma}_i> = 0 & >\overline{\sigma}_i <= \overline{\sigma}_i \end{array} \quad \text{and} \quad \begin{array}{l} \text{when} \\ \end{array} \quad \begin{array}{l} \overline{\sigma}_i > 0 \\ \overline{\sigma}_i \leq 0 \end{array} \tag{25}$$

Compute the equivalent stresses from

$$\overline{\sigma}^{-} = \sum_{i=1}^{3} > \overline{\sigma}_i < \text{ and } \tilde{\sigma}^{-} = \sqrt{\sum_{i=1}^{3} (> \overline{\sigma}_i <)^2} \tag{26}$$

and the strains vector from effective stresses vector by

$$\left\{\overline{\varepsilon}^{+}\right\} = [C]^{-1}\left\{< \overline{\sigma}_i >\right\} \text{ και } \left\{\overline{\varepsilon}^{-}\right\} = [C]^{-1}\left\{> \overline{\sigma}_i <\right\} \tag{27}$$

where [C] is the elasticity matrix.

Step3

Compute the parameters α^{+} and α^{-} from

$$\begin{aligned} \alpha^{+} &= \min\left[\tfrac{2k^{+}+k^{-}}{2k^{+}}, 1\right] \\ \alpha^{-} &= \min\left[\tfrac{k^{+}+k^{-}}{k^{-}}, 1\right] \end{aligned} \tag{28}$$

where

$$\begin{aligned} k^{+} &= \sum_{i=1}^{3} H_i^{+} \frac{\overline{\varepsilon}_i^{+}\left(\overline{\varepsilon}_i^{+} + \overline{\varepsilon}_i^{-}\right)}{\left(\tilde{\varepsilon}^{+}\right)^2} \\ k^{-} &= \sum_{i=1}^{3} H_i^{-} \frac{\overline{\varepsilon}_i^{-}\left(\overline{\varepsilon}_i^{+} + \overline{\varepsilon}_i^{-}\right)}{\left(\tilde{\varepsilon}^{-}\right)^2} \end{aligned} \tag{29}$$

with

$$\begin{matrix} H_i^{+} = 1 \\ H_i^{+} = 0 \end{matrix} \text{ and } \begin{matrix} H_i^{-} = 0 \\ H_i^{-} = 1 \end{matrix} \text{ when } \begin{matrix} \left(\overline{\varepsilon}_i^{+} + \overline{\varepsilon}_i^{-}\right) > 0 \\ \left(\overline{\varepsilon}_i^{+} + \overline{\varepsilon}_i^{-}\right) \le 0 \end{matrix} \tag{30}$$

Step4

Compute the scalar norms τ^{+} and τ^{-} of undamaged stress state from

$$\overline{\tau}^{+} = \sqrt{\left\{< \overline{\sigma} >\right\}^T \left[C^{-1}\right]\left\{< \overline{\sigma} >\right\}} \tag{31}$$

and

$$\overline{\tau}^{-} = \sqrt{\sqrt{3}(K\overline{\sigma}_{oct}^{-} + \overline{\tau}_{oct}^{-})} \tag{32}$$

where

$$K = \sqrt{2}\frac{1-R_0}{1-2R_0} \tag{33}$$

with

$$R_0 = \frac{f_{c-2D}}{f_{c-1D}} = \frac{\textit{biaxial compressive strength}}{\textit{uniaxial compressive strength}} \tag{34}$$

Step5

Compute the damage indices

$$d^{+} = 1 - \frac{r_0^{+}}{\overline{\tau}^{+}} e^{A^{+}\left(1-\frac{\overline{\tau}^{+}}{r_0^{+}}\right)} \tag{35}$$

and

$$d^{-} = 1 - \frac{r_0^{-}}{\overline{\tau}^{-}}(1-A^{-}) - A^{-} e^{B^{-}\left(1-\frac{\overline{\tau}^{-}}{r_0^{-}}\right)} \tag{36}$$

where A^{+}, A^{-} and B^{-} are material parameters (Faria and Oliver 1993, Hatzigeorgiou 2001). Furthermore, r_0^{+} and r_0^{-} correspond to the beginning of damage where

$$r_0^{+} = \frac{f_t}{\sqrt{E}} \tag{37}$$

and

$$r_0^{-} = \sqrt{\sqrt{\frac{2}{3}}\frac{R_0}{1-2R_0} f_c} \tag{38}$$

The damage indices of Eq. (33) and (34) are unified in one and only damage index d as

$$d = \alpha^{+} d^{+} + \alpha^{-} d^{-} \tag{39}$$

It is worth noticing that the superscripts $(+)$ and $(-)$ correspond to tension and compression, respectively. The stress-strain diagram in uniaxial conditions and the damage bounding surface in biaxial conditions of FOM model appear in Fig. 5.

It is observed that this model is capable of taking into account the biaxiality effect in compression. In conclusion, Oñate's model is characterized by a great simplicity but its use is mostly suggested in tension dominated states of deformation, while the FOM model, despite its complexity is capable of simulating any deformation state.

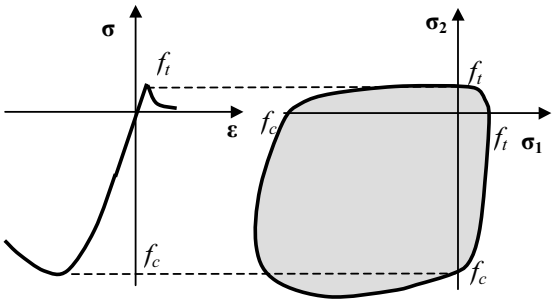

Figure 5 : FOM model representation

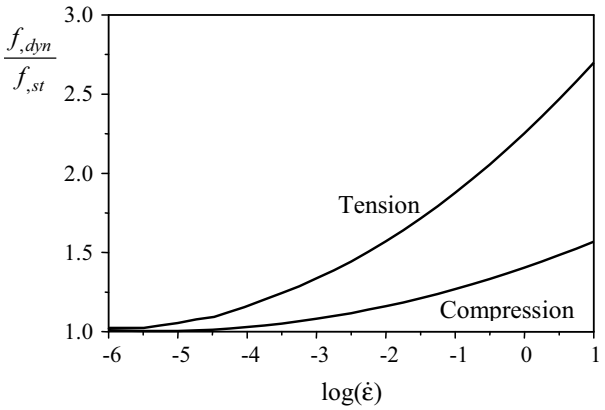

Figure 6 : Dynamic to static strengths ratios

4.3 Strain rate dependency

The sensitivity of the mechanical behavior of concrete (or other quasi-brittle materials) to the rate of external loading is a well known fact. This feature is taken into account by a simple and general methodology proposed here in, which appears stepwise below:

Step1

Compute the tensile $\dot{\varepsilon}^+$ and compressive $\dot{\varepsilon}^-$ strain rate between the present (n+1) and the previous (n) time step from

$$\dot{\varepsilon}^+ = \left| \frac{(\tilde{\varepsilon}^+ \hat{\varepsilon}^+)_{n+1} - (\tilde{\varepsilon}^+ \hat{\varepsilon}^+)_n}{t_{n+1} - t_n} \right|, \; \dot{\varepsilon}^- = \left| \frac{(\tilde{\varepsilon}^- \hat{\varepsilon}^-)_{n+1} - (\tilde{\varepsilon}^- \hat{\varepsilon}^-)_n}{t_{n+1} - t_n} \right| \tag{40}$$

Step2

Compute the dynamic tensile $f_{t,\mathrm{dyn}}$ and compressive $f_{c,\mathrm{dyn}}$ strength for the above strain rates. In this work, the experimental results of Suaris & Shah (1985) providing the ratios $f_{t,\mathrm{dyn}}/f_{t,\mathrm{st}}$ and $f_{c,\mathrm{dyn}}/f_{c,\mathrm{st}}$ versus strain rate have been adopted. This work uses the Suaris & Shah (1985) curves in analytic forms

$$\frac{f_{t,\mathrm{dyn}}}{f_{t,\mathrm{st}}} = 2.253 + 0.411 \left[\log\left(\dot{\varepsilon}^+\right)\right] + 0.035 \left[\log\left(\dot{\varepsilon}^+\right)\right]^2 \tag{41}$$

and

$$\frac{f_{c,\mathrm{dyn}}}{f_{c,\mathrm{st}}} = 1.405 + 0.150 \left[\log\left(\dot{\varepsilon}^-\right)\right] + 0.014 \left[\log\left(\dot{\varepsilon}^-\right)\right]^2 \tag{42}$$

which have been obtained here in by a polynomial regression.

The ratios between dynamic and static, tensile and compressive strength versus strain rate appear in Fig. 6.

Step3

Replace in Oñate's and FOM models the static values of tensile and compressive strengths with the corresponding dynamic values, for every time step.

For more details one can consult Hatzigeorgiou (2001) and Hatzigeorgiou, Beskos, Theodorakopoulos and Sfakianakis (2001).

5 Examples

This section describes three representative numerical examples in order to illustrate the use and demonstrate the advantages of the proposed three-dimensional dynamic damage boundary element method of analysis.

5.1 Dynamic tensile loading of a concrete bar

The ability of the proposed methodology to simulate a concrete bar under dynamic uniaxial tension is examined in this example. The dimensions of the bar are $20\times1\times1$ m, while its geometry and discretization appear in Fig. 7. Cervera, Oliver and Manzoli (1995) using the finite element method have also investigated this example. The material parameters for this analysis, using the Oñate's damage model are:

- modulus of elasticity E = 30.0 GPa,

- density ρ = 2400 kg/m^3,
- Poisson ratio ν = 0.18,
- uniaxial compressive strength f_c = 30.0 MPa,
- uniaxial tensile strength f_t = 3.0 MPa and
- fracture energy G_f = 250.0 N/m.

The concrete bar is subjected to a dynamic uniaxial tensile displacement varying linearly with time and with 10^{-6}, 10^{-2} and 10^{-1} sec^{-1} strain rates. Figure 8 shows the stress-strain curves for these strain rates. A very good convergence is evident between the analysis with the proposed BEM and the FEM results of Cervera, Oliver and Manzoli (1995).

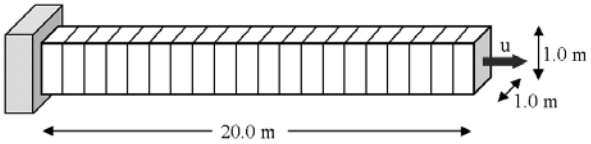

Figure 7 : Geometry and discretization of Example 1

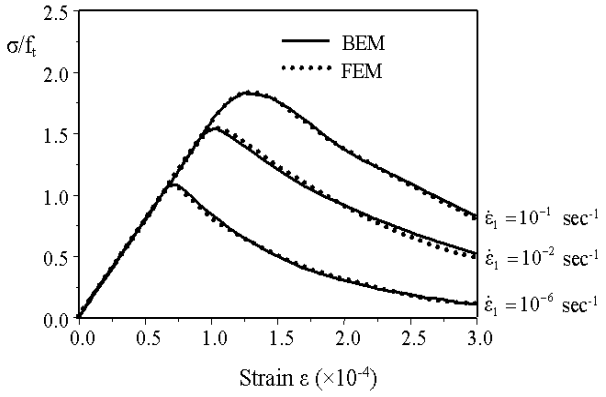

Figure 8 : Concrete bar under dynamic tensile loading. Stress-strain curves under various strain rates

5.2 Dynamic compressive loading of a concrete specimen

This example presents numerical simulations of a concrete specimen under dynamic uniaxial compression. The specimen dimensions are 20×20×5 cm. The geometry and the discretization appear in Fig. 9.

This example undertakes to simulate the experimental tests of Suaris and Shah (1985) using the proposed methodology in conjunction with the FOM damage model. The material parameters for the analysis are:

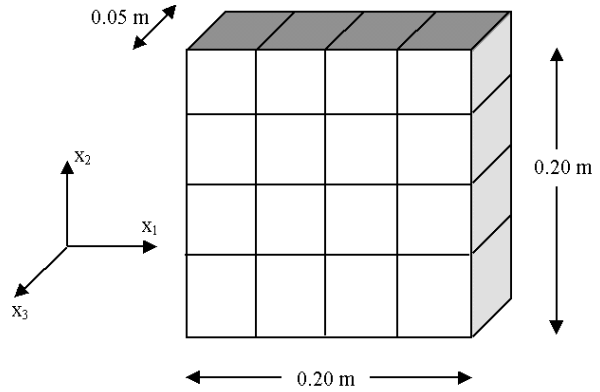

Figure 9 : Geometry and discretization of Example 2

- modulus of elasticity E = 33.0 GPa,
- density ρ = 2400 kg/m^3,
- Poisson ratio ν = 0.18,
- compressive elastic limit f_0 = 10.0 MPa,
- uniaxial compressive strength f_c = 47.5 MPa,
- uniaxial tensile strength f_t = 4.0 MPa,
- biaxial to uniaxial compressive strength R_0 = 1.16 and
- fracture energy G_f = 150.0 N/m.

The concrete specimen is subjected to a dynamic uniaxial compressive displacement varying linearly with time and with 10^{-6} and 0.088 sec^{-1} strain rates. Figure 10 shows the stress-strain curves for these strain rates. A very good convergence is evident between analytical and experimental results.

5.3 Dynamic analysis of a mortar beam

In this example, a simply supported mortar beam subjected to a central impact loading is analyzed numerically by the proposed method using the Oñate's model. The material parameters are

- modulus of elasticity E=22000.0 N/mm^2
- Poisson ratio ν=0.15
- uniaxial tensile strength f_t=3.91 N/mm^2
- uniaxial compressive strength f_c=35.0 N/mm^2
- density ρ=2410 kg/m^3
- fracture energy G_f =103.7 N/m.

Figure 11 contains the geometry and the 3-D BEM discretization of the structure. Due the symmetry only half of the beam is discretized.

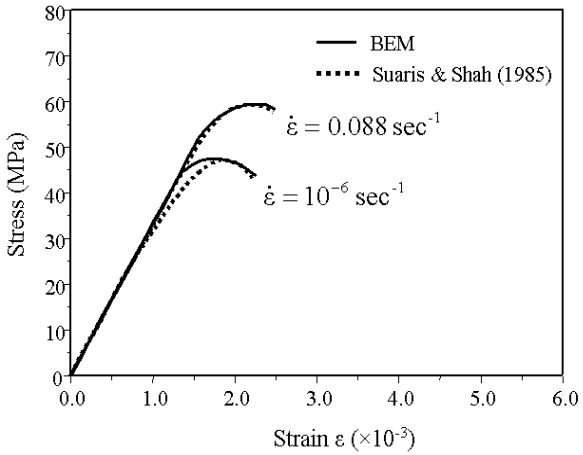

Figure 10 : Concrete bar under dynamic compressive loading. Stress-strain curves under various strain rates

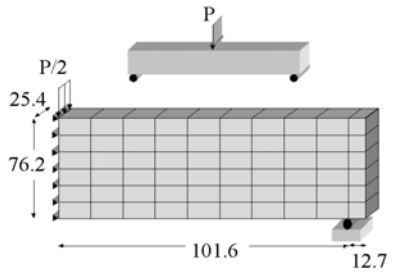

Figure 11 : Geometry and discretization of Example 3 (dimensions in mm)

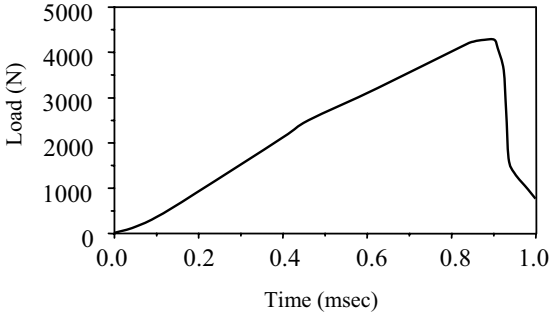

Figure 12 : Loading history on Example 3

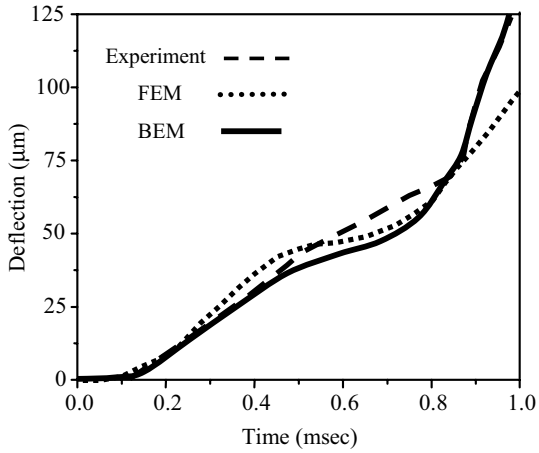

Figure 13 : Time history of deflection at load point

Figure 12 shows the loading history, applied at the upper central line of the beam.

Figure 13 depicts the time history of the vertical displacement at the load point. The proposed BEM exhibits a very good agreement with the experimental and the FEM results of Du, Kobayashi and Hawkins (1989).

6 Conclusions

In this paper a BEM for transient dynamic inelastic analysis of 3-D solids and structures is presented. The method employs the static fundamental solution of the problem and this creates not only boundary integrals but also volume integrals as well due to the presence of inelasticity and inertial effects. Thus, boundary as well as domain (interior) elements are used in the space discretization of the problem. The implicit algorithm of Houbolt is employed for the numerical integration in time. Initial stress formulation and damage theories are used to simulate inelastic material behavior, including strain rate effects. The main aspects concerning the numerical implementation required for the solution of the nonlinear dynamic problem are also presented. Three numerical examples are described to illustrate the method and demonstrate its accuracy. Finally, it is worth noticing that the three-dimensional treatment of dynamic inelastic problems requires a considerable computational effort.

Acknowledgement: Funding by the General Secretariat of Research and Technology of Greece and the Public Power Corporation of Greece under Contract Number YPER94 #371 are gratefully acknowledged. The authors also are thankful to Professor E. Oñate for furnishing to them various references on damage theory.

References:

Banerjee, P.K. (1994): *The Boundary Element Methods in Engineering*, Mc Graw-Hill, U.K.

Ahmad, S.; Banerjee, P.K. (1990): Inelastic transient dynamic analysis of three-dimensional problems by BEM, *Int. J. Num. Meth. Engng*, vol. 29, pp. 371-390.

Bazant, Z.P.; Planas, J. (1998): *Fracture and Size Effect in Concrete and Other Quasi-Brittle Materials*, CRC Press, Florida.

Beskos, D.E. (1995): Dynamic inelastic structural analysis by boundary element method, *Arch. Comput. Meth. Engng*, vol. 2, pp. 55–87.

Beskos, D.E. (1997): Boundary element methods in dynamic analysis: Part II (1986-1996), Appl. Mech. Rev. ASME, vol. 50, pp. 149-197.

Bu, S. (1997): Infinite boundary elements for the dynamic analysis of machine foundations, *Int. J. Num. Meth. Engng*, vol. 40, pp. 3901-3917.

Carrer, J.A.M.; Telles, J.F.C. (1992); A boundary element formulation to solve transient dynamic elastoplastic problems, *Comput. & Struct.*, vol. 45, pp. 707-713.

Cerrolaza, M.; Garcia R. (1997): Boundary elements and damage mechanics to analyze excavations in rock mass, *Engng Anal. Bound. Elem.*, vol. 20, pp. 1-16.

Cervera, M.; Oliver, J.; Manzoli, O. (1996): A rate-dependent isotropic damage model for the seismic analysis of concrete dams, *Earth. Engng Struct. Dyn.*, vol. 25, pp. 987-1010.

Du, J.; Kobayashi, A.S.; Hawkins, N.M. (1989): FEM dynamic fracture analysis of concrete beams, *J. Engng Mech.*, ASCE, vol. 115, 10, pp. 2136-2149.

Faria, R.; Oliver, X. (1993): *A Rate Dependent Plastic-Damage Constitutive Model for Large-Scale Computations in Concrete Structures*, Monografia No 17, CIMNI, Barcelona, Spain.

Frangi A.; Maier, G. (1999): Dynamic elastic-plastic analysis by a symmetric Galerkin boundary element method with time-independent kernels, *Comp. Meth. Appl. Mech. Engng*, Vol. 171, pp. 281-308.

Garcia, R.; Florez-Lopez, J.; Cerrolaza, M. (1999): A boundary element formulation for a class of non-local damage models, *Int. J. Solids Struct.*, vol. 36, 24, pp. 3617-3638.

Guiggiani, M.; Gigante, A. (1990): A general algorithm for multidimensional Cauchy principal value integrals in the boundary element method, *J. Appl. Mech.*, vol. 57, pp. 906-915.

Hatzigeorgiou, G.D. (2001): *Seismic Inelastic Analysis of Underground Structures by Means of Boundary and Finite Elements*, Ph.D. Thesis (in Greek), University of Patras.

Hatzigeorgiou, G.D.; Beskos, D.E. (2002a): Dynamic elastoplastic analysis of 3-D Solids and Structures by the D/BEM, *Comp. Struct.*, vol. 80, pp. 339-347.

Hatzigeorgiou, G.D.; Beskos, D.E. (2002b): Static analysis of 3-D damaged solids and structures by BEM, *Engng Anal. Bound. Elem.*, vol. 26, pp. 521-526.

Hatzigeorgiou, G.D.; Beskos, D.E.; Theodorakopoulos, D.D.; Sfakianakis, M. (2002): A simple concrete damage model for dynamic FEM applications, *Int. J. Comp. Engng. Sci.*, vol. 2, pp. 267-286.

Herding, U.; Kuhn, G. (1996): A field boundary element formulation for damage mechanics, *Engng Anal. Bound. Elem.*, vol. 18, .2, pp. 137-147.

Karabalis, D.L.; Beskos, D.E. (1997): Numerical methods in earthquake engineering, in *Computer Analysis and Design of Earthquake Resistant Structures : A Handbook*, D.E. Beskos and S.A. Anagnostopoulos, Editors, Computational Mechanics Publications, Southampton.

Kogl, M.; Gaul, L. (2000): A 3-D boundary element method for dynamic analysis of anisotropic elastic solids, Comp. Model. Engng. Sci, vol. 1, pp.27-44.

Kontoni, D.P.N.; Beskos, D.E. (1993): Transient dynamic elastoplastic analysis by the dual reciprocity BEM, *Engng Anal. Bound. Elem.*, vol. 12, pp. 1-16.

Krajcinovic, D. (1996): *Damage Mechanics*, Elsevier Science, Amsterdam.

Maier, G.; Pollizzotto C. (1987): A Galerkin approach to boundary element elastoplastic analysis, *Comp. Meth. Appl. Mech. Engng*, vol. 60, pp. 175-194.

Mazars, J. (1986): A description of micro- and macroscale damage on concrete structures, *Engng. Fracture Mech.*, vol. 25, 5-6, pp. 729-737.

Oñate, E. (1997): *Reliability Analysis of Concrete Structures. Numerical and Experimental Studies*, CIMNE, No. 107, Barcelona, Spain.

Providakis, C.P.; Beskos, D.E. (1994): Dynamic analysis of elasto-plastic flexural plates by the D/BEM, *Engng Anal. Bound. Elem.*, vol.14, 1, pp. 75-80.

Providakis, C.P.; Beskos, D.E. (1999): Dynamic analysis of plates by boundary elements, *Appl. Mech. Rev.*, vol. 52, 7, pp. 213-236.

Rajgelj, S.; Amadio, S.; Nappi, A. (1992): Application of damage mechanics concepts to the boundary element method, in *Boundary Element Technology VII*, ed. Brebbia, C.A. and Ingber, M.S., Elsevier, London, pp. 617-634.

Sellers, E.; Napier, J. (1997): A comparative investigation of micro-flaw models for the simulation of brittle fracture in rock, *Comput. Mech.*, vol. 20, 1-2, pp. 164-169.

Siebrits, E.; Peirce, A.P. (1997): Implementation and application of elastodynamic boundary element discretizations with improved stability properties, *Engng Comput.*, vol. 14, 6, pp. 669-91.

Suaris, W.; Shah, S. (1985): Constitutive model for dynamic loading of concrete, *J. Stuct. Engng*, ASCE, vol. 111, pp. 563-576.

Telles, J.C.F.; Brebbia, C.A. (1979): On the application of the boundary element method to plasticity, *App. Math. Modeling*, vol. 3, pp. 466-470.

Telles, J.F.C.; Carrer, J.A.M. (1994): Static and transient dynamic nonlinear stress analysis by the boundary element method with implicit techniques, *Engng Anal. Bound. Elem.*, vol. 14, pp. 65-74.

Telles, J.C.F.; Carrer, J.A.M.; Mansur, W.J. (1999): Transient dynamic elastoplastic analysis by the time-domain BEM formulation, *Engng Anal. Bound. Elem.*, vol. 23, 5-6, pp. 479-486.

Zienkiewicz O.C.; Taylor, R.L. (1991): The *Finite Element Method*, Vol. II, 4th edition, Mc Graw Hill, London.